THE ASTROPHYSICAL JOURNAL, 579:L13–L16, 2002 November 1

THE PUZZLINGLY SMALL Ca II TRIPLET ABSORPTION IN ELLIPTICAL GALAXIES

R. P. SAGLIA, CLAUDIA MARASTON, DANIEL THOMAS, AND RALF BENDER
Universitäts-Sternwarte München, Scheinerstrasse 1, D-81679 Munich, Germany; and Max-Planck-Institut für extraterrestrische Physik, Postfach 1312, D-85741 Garching, Germany; saglia@usm.uni-muenchen.de, maraston@usm.uni-muenchen.de, daniel@usm.uni-muenchen.de, bender@usm.uni-muenchen.de
AND
MATTHEW COLLESS
Research School of Astronomy and Astrophysics, Australian National University, Weston Creek, ACT 2611, Australia; colless@mso.anu.edu.au
Received 2002 August 9; accepted 2002 September 17; published 2002 September 30

ABSTRACT

We measure the central values (within $R_e/8$) of the Ca II triplet line indices CaT* and CaT and the Paschen index PaT at 8600 Å for a 93% complete sample of 75 nearby early-type galaxies with $B_T < 12$ mag and $V_{\rm gal} < 2490$ km s^{-1}. We find that the values of CaT* are constant to within 5% over the range of central velocity dispersions 100 km s^{-1} $\leq \sigma \leq$ 340 km s^{-1}, while the PaT (and CaT) values are mildly anticorrelated with σ. Using simple and composite stellar population models, we show the following: (1) The measured CaT* and CaT are lower than expected from simple stellar population (SSP) models with Salpeter initial mass functions (IMFs) and with metallicities and ages derived from optical Lick (Fe, Mg, and Hβ) indices. Uncertainties in the calibration, the fitting functions, and the SSP modeling taken separately cannot explain the discrepancy. On average, the observed PaT values are within the range allowed by the models and the large uncertainties in the fitting functions. (2) The steepening of the IMF at low masses required to lower the CaT* and CaT indices to the observed values is incompatible with the measured FeH index at 9916 Å and the dynamical mass-to-light ratios of elliptical galaxies. (3) Composite stellar populations with a low-metallicity component reduce the disagreement, but rather artificial metallicity distributions are needed. Another explanation may be that calcium is indeed underabundant in elliptical galaxies.

Subject headings: galaxies: elliptical and lenticular, cD — galaxies: fundamental parameters

1. INTRODUCTION

The determination of the mean ages and metallicities of local elliptical galaxies is one of the key observational tests of models for galaxy formation and evolution. The classical picture of monolithic collapse (Larson 1974) assumes high formation redshifts and passive evolution, producing large central metallicities with strong gradients. In contrast, semianalytic models of galaxy formation embedded in the hierarchical structure formation typical of cold dark matter universes (Kauffmann 1996) produce elliptical galaxies through mergers of disks and predict a large spread in the formation ages (especially for field elliptical galaxies), with solar mean metallicities and shallow gradients. Although many indications support the merging scenario, a clear-cut answer from the observations has been hampered by the age-metallicity degeneracy in the spectra of (simple) stellar populations: the same broadband colors and absorption features can be obtained for very different combinations of ages and metallicities. The combined use of indices more sensitive to age (like the Balmer lines) and those more sensitive to metallicity (like Mg_2 and Fe5270 and Fe5335) offers a way out (Worthey 1994). However, ambiguities remain, because the presence of a small metal-poor old stellar population may bias the age estimate (Maraston & Thomas 2000, hereafter MT), and the metallicity estimate based on the Mg indices are systematically higher than the ones using iron lines (the so-called Mg over Fe overabundance problem; Worthey, Faber, & González 1992; Trager et al. 2000; Thomas, Maraston, & Bender 2002, hereafter TMB). Recent modeling of the Ca II triplet line at 8600 Å (Idiart, Thévenin, & De Freitas Pacheco 1997, hereafter I97; García-Vargas, Mollá, & Bressan 1998; Mollá & García-Vargas 2000) concluded that this index is insensitive to age for populations older than 1 Gyr, raising hopes that it could allow a robust measure of metallicity and, in combination with colors or indices, age. An excellent review of the literature on the subject can be found in Cenarro et al. (2001a, hereafter C01).

Here we present the results of our survey of the Ca II triplet line in local elliptical galaxies in the light of the new definition of the index given by C01 and their accurate determination of its stellar calibrators (the so-called fitting functions [FFs]; Cenarro et al. 2001b, 2002, hereafter C02). In § 2, we describe the observations and the data reduction, and in § 3 we present the data, discuss them with new stellar population models, and draw our conclusions.

2. OBSERVATIONS AND DATA REDUCTION

We observed the Ca II triplet region at 8600 Å along the major axis of 94 early-type elliptical galaxies from the Faber et al. (1989, hereafter F89) catalog. The results presented in this Letter are based on the subsample with $B_T < 12$ mag and $V_{\rm gal} < 2490$ km s^{-1}, where we observed 75 galaxies, reaching 93% completeness. At $V_{\rm gal} \approx 2500$ km s^{-1}, the reddest window of the indices considered here moves into a region of strong sky emission lines, making the measurements sensitive to sky subtraction errors.

The observations were performed at the 3.5 m Calar Alto in 2001 February and April, the La Silla ESO New Technology Telescope in 2001 May and November, and the Siding Spring 2.3 m telescope in 2001 May and October and 2002 January, with instrumental resolution ranging from 70 to 80 km s^{-1}. Details will be presented in R. P. Saglia et al. (2002, in preparation). Typically, two spectra along the major axis of the galaxy were obtained with summed exposure times ranging between 1 and 3 hr. Template stars used in the determinations of the FFs of C01 were also observed, trailed along the slit. The standard CCD data reduction was carried out under the image processing package MIDAS provided by ESO. A de-

tailed description of the procedure can be found in R. P. Saglia et al. (2002, in preparation). The wavelength calibration procedure achieved 0.1 Å rms precision. The systematic residuals after sky subtraction, estimated from the blank sky frames, are less than 1%.

The galaxy kinematics were derived using the Fourier correlation quotient method (Bender 1990) following Bender, Saglia, & Gerhard (1994). The line indices were measured following the prescriptions of C01 for the computation of the newly defined "generic" indices CaT, PaT, and $\mathrm{CaT}^* = \mathrm{CaT} - 0.93\mathrm{PaT}$. In summary, generic indices have an arbitrary number of continuum and spectral feature bandpasses and the pseudocontinuum is derived by using an error-weighted least-squares fit to all the pixels of the continuum bands. The CaT index measures the combined strength of the Ca1, Ca2, and Ca3 lines similar to Díaz, Terlevich, & Terlevich (1989) and I97 and has a possible contribution for the Paschen lines P16, P15, and P13. The PaT index measures the combined strength of the Paschen lines P17, P14, and P12. The CaT* measures the strength of the Ca II triplet corrected for the contamination from Paschen lines. At our resolution (see below), we found no significant difference in the measurements, if the flux calibration (performed by C01) was applied or not.

The statistical errors were derived from Monte Carlo simulations, which also take into account the uncertainties from the kinematics through the redshift and the broadening correction. The errors from systematics in the sky subtraction (in general, at the 1% level; see above) were found to dominate in the outer parts of the galaxies. The procedure described in Mehlert et al. (1998) was followed to achieve a uniform focus with wavelength, when necessary. A correction for the broadening of the lines due to the internal kinematics of the galaxies was applied to scale the indices to the instrumental resolution, using a K-type stellar template. As discussed by C01, this correction is spectral type dependent and therefore somewhat uncertain; it is small ($\lesssim$5%) for the CaT and CaT* indices but as large as 20% at $\sigma \approx 300$ km s^{-1} for the PaT index. The uncertainties in the correction are $\approx$0.1 Å. Finally, since the C01 system is based on stellar spectra taken with 22 km s^{-1} resolution, nearly a factor 4 higher than the present observations, the data set was calibrated on this system by comparing the values of the indices for the template stars in common and applying linear corrections to the CaT and PaT indices. Central values of the velocity dispersion σ and of the indices were derived by averaging the profiles within $R_e/8$ (with R_e taken from F89), luminosity-weighting the data points. The typical statistical errors on the central indices are smaller than 0.1 Å. The rms of the differences of the central values of the galaxy repeats is 0.2 Å, having applied a 0.3 Å correction to one of the runs.

3. RESULTS AND DISCUSSION

Figure 1 shows the relation between the CaT*, PaT, and CaT indices as a function of the central velocity dispersion. As already noted by Cohen (1979), Faber & French (1980), and Terlevich, Díaz, & Terlevich (1990), elliptical galaxies have very similar central values of the calcium triplet index. Averaged over the galaxy sample, the CaT* has a mean of 6.93 Å and an rms of 0.33 Å, or $\approx$5%, just above the measurement errors (statistical, systematic, and owing to calibration). Within the derived errors, the CaT* index does not depend on σ, while a mild anticorrelation is observed for both PaT and CaT, driven by the slightly larger PaT at lower sigmas. This contrasts with the behavior of the

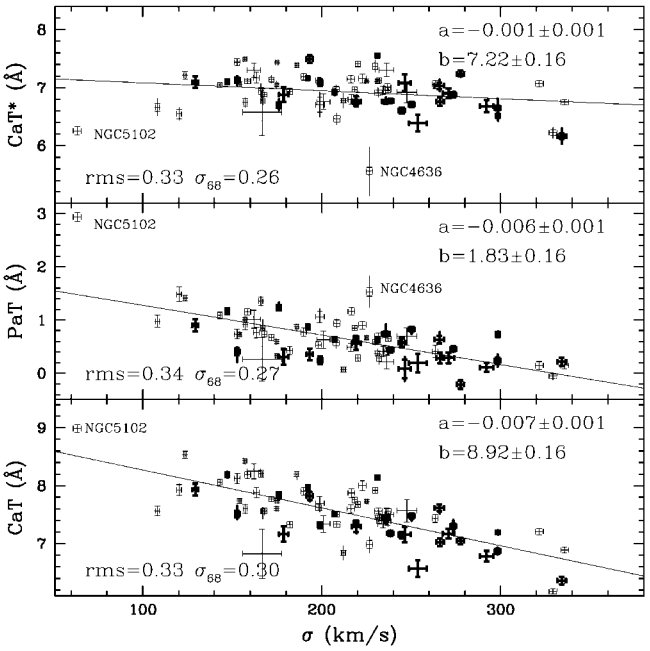

FIG. 1.—Relation between the central velocity dispersion (averaged within $R_e/8$) and the CaT*, PaT, and CaT indices. The galaxies appearing also in Fig. 2 are thick. Error bars show the statistical errors. Systematic errors due to sky subtraction of $\pm 1\%$ exceeding the statistical errors are indicated by prolonging the error bars beyond the horizontal mark. The two most deviant galaxies are labeled. The lines show least-square fits to the data points. Labels give their (*a*) slopes and (*b*) zero points, the derived errors, the rms about the best fits, and its robust determination (at 68% of the cumulative distribution of the residuals).

Mg_2 and Mg *b* line indices, known to correlate strongly with σ in elliptical galaxies (Bender, Burstein, & Faber 1993; Colless et al. 1999). These indices trace the α-element magnesium (Tripicco & Bell 1995; Maraston et al. 2002), and if the Ca II triplet indices were to trace the calcium abundance, also an α-element, a correlation with σ could have been expected.

Figure 2 shows stellar population models of the CaT*, PaT, and CaT indices constructed using the FF subroutines of C02 and the updated code of Maraston (1998, hereafter M98). A detailed description of the models considered here will be given in C. Maraston et al. (2002, in preparation). The black lines show simple stellar population (SSP) models with the Salpeter initial mass function (IMF) as a function of age and metallicity. These models reproduce well the tight metallicity-CaT correlation observed for globular clusters (*open blue squares*; from Armandroff & Zinn 1988, transformed using the relation given by C01; [*Z*/H] from Harris 1996). At metallicities higher than solar, the models flatten and the age dependence becomes more important. The PaT index varies strongly with age for ages less than a few gigayears. It reaches a value of $\approx$1 Å at high ages. Note, however, the large rms uncertainties of the FFs ($\approx$0.4 Å).

The blue filled circles show the subsample of the database investigated here where ages and metallicity estimates are available from the analysis of the Fe, Mg, and Hβ Lick indices (TMB). The results discussed in the following do not change if the set of ages and metallicities of Terlevich & Forbes (2002) are used instead. The same applies to the effects of errors on the age, metallicity, and index, explored using Monte Carlo simulations. Within the large uncertainties allowed by the FFs, the models reproduce the average value of the measured PaT indices.

In contrast, the models predict values of CaT* and CaT more than 1 Å larger than the measured ones. Such a large discrepancy

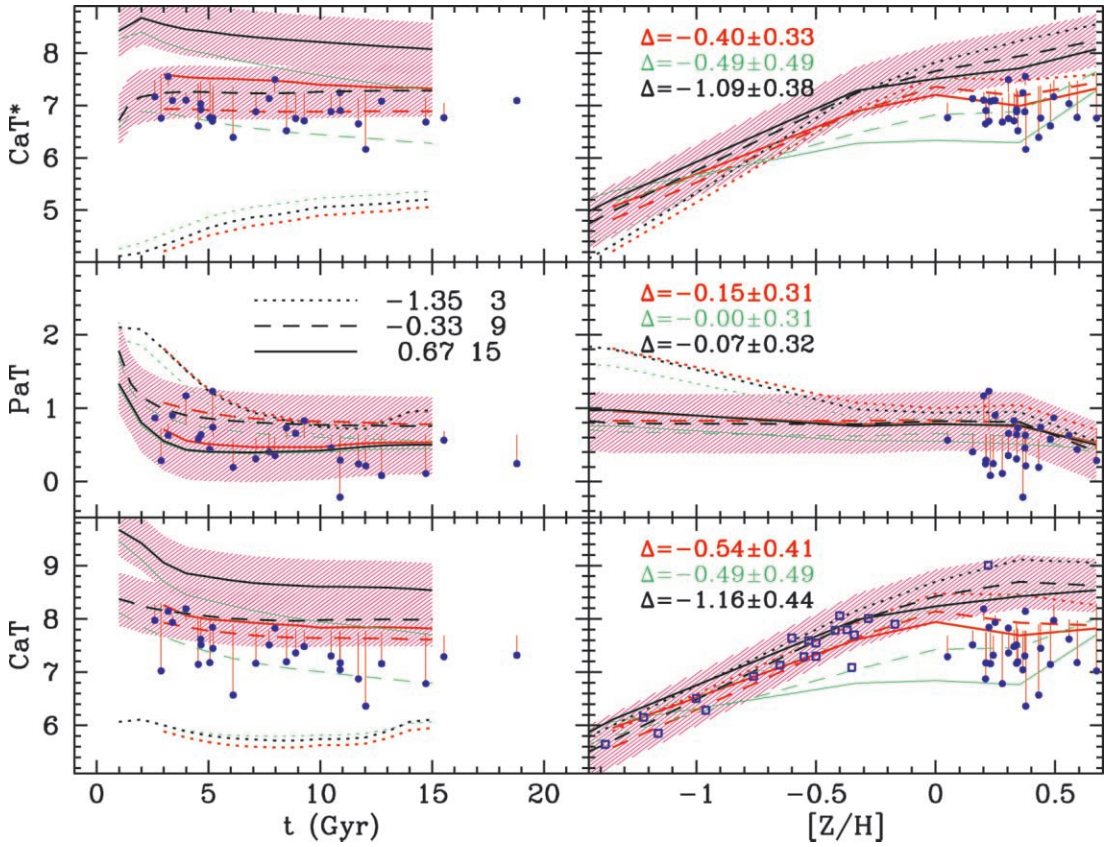

FIG. 2.—Stellar population models of the CaT*, PaT, and CaT indices as a function of age (*left panel*) and metallicity (*right panel*). The black lines show SSPs with a Salpeter ($\alpha = -2.35$) IMF. The magenta shaded areas centered on the [Z/H] = 0.67, −1.35 and $t = 9$ lines show the range allowed by the uncertainties in the FFs. The green lines show SSPs with IMF slope $\alpha = -4$ for $M < 0.6\ M_{\odot}$ and $\alpha = -2.35$ at larger masses. The red lines show composite stellar population models, where 10% of the mass has low metallicity ([Z/H] = −2.25). The different line types show different metallicities (*left panel*) and ages (*right panel*), as given in the key in the left middle panel. The blue filled circles show the galaxy sample, with ages and metallicities determined from Lick indices (see text). The vertical red bars point to the predicted values of the CSP models with a low-metallicity component. The mean differences Δ and rms between measured and predicted values are given color-coded as above in the labels.

cannot be explained by calibration errors, which are at least a factor of 5 smaller. Uncertainties in the FFs (rms ≈ 0.5 Å) alone seem also unable to explain it, although at high metallicities ([Z/H] > 0.3) the FFs are based on only a handful of stars. The CaT* of a high-Z SSP is dominated by the contribution of the red giant branch and the red clump (RC). If we set artificially the value of the CaT* FF at [Z/H] = 0.35 from the giant branch phase on to 8 Å (the lowest value measured for stars in this phase; most of the stars have CaT* = 9–10 Å), we obtain CaT* = 7.5 Å for the SSP, still 0.5 Å larger than what is observed in elliptical galaxies. The flux contribution of the RC can vary within ≈30% owing to the uncertainties on the lifetime of this phase (Zoccali et al. 2000a). If we reduce the flux of the RC by this amount, we again obtain CaT* = 7.5 Å for the SSP. Only a 50% reduction would produce CaT* ≈ 7 Å.

The SSP Salpeter models translate the averaged observed value of the CaT* into [Z/H] = −0.5 ± 0.1, or $Z = 0.3 \pm 0.1\ Z_{\odot}$. Taking this result at face value, if the CaT* traces the calcium abundance, this could indicate that this element is underabundant, a suggestion already put forward by Peletier et al. (1999) considering three elliptical galaxies. A similar effect has been suggested by McWilliam & Rich (1994) and Rich & McWilliam (2000), who analyze a sample of metal-rich bulge stars, suggesting that while Mg and Ti are overabundant with respect to Fe, Ca and Si have nearly solar ratios. In addition, modeling the Ca4227 Lick index, TMB find [Ca/Mg] ≈ −0.3 in elliptical galaxies (see also Vazdekis et al. 1997). However, the issue of Ca underabundance in high-metallicity stars is still controversial (McWilliam 1997); C02 point out that the CaT index does not correlate with the [Ca/Fe] stellar overabundance, and current modeling of the yields of Type II supernovae (Woosley & Weaver 1995) does not allow much room in this direction. While Mg (and O) are produced in the greatest quantities in high-mass stars (≈35 $M_{\odot}$), lower mass stars (≈15–25 $M_{\odot}$) are responsible for the production of Ca (and Si). An IMF biased to the high masses or extremely short (≈10^7 yr) star formation bursts that avoid the Ca enrichment at high metallicities, as discussed by Mollá & García-Vargas (2000), do not seem a very appealing solution.

An alternative explanation of the low value of the CaT* index could be a steeper IMF at low stellar masses, since the CaT* index decreases with increasing gravity for cool stars. The green lines of Figure 2 show SSP models with IMF slope $\alpha = -4$ for $M < 0.6\ M_{\odot}$ and $\alpha = -2.35$ (Salpeter) at larger masses. The CaT* and CaT indices at the high metallicities have a stronger dependence on age and are indeed able to reproduce the measured values of elliptical galaxies. However, the observational evidence points to an IMF flatter than Salpeter in the bulge of our Galaxy (Zoccali et al. 2000b). In addition, as already discussed by Carter, Visvanathan, & Pickles (1986) and Couture & Hardy (1993), such dwarf-dominated models produce values of the FeH feature at 9916 Å that are an order of magnitude larger than what is observed. Moreover, the visual mass-to-light ratios (at $t = 10$ Gyr, $Z = Z_{\odot}$, one gets $M/L_B = 40\ M_{\odot}/L_{\odot}$;

M98) are incompatible with dynamical estimates (Gerhard et al. 2001; $M/L_B \approx 6$).

Since at low metallicity the CaT* and CaT indices depend strongly on Z (see Fig. 2), composite stellar populations (CSPs) with a low-metallicity component are bound to produce (significantly) lower CaT* and CaT indices than SSPs with the same (high) mean metallicity, while leaving the PaT values essentially unchanged. The red lines of Figure 2 explore this case, presenting CSPs where 90% of the mass is an SSP model and 10% is the $[Z/H] = -2.25$ SSP with the same age, as done in MT. They show that this admittedly rather artificial model is compatible with the UV constraints available for elliptical galaxies, generating at the same time higher values of the Hβ index than SSPs of the same metallicity. The CSP models of Figure 2 predict almost constant values of the CaT* and CaT indices for $Z \geq Z_{\odot}$. This stems from the increasing relative importance of the flux at 8600 Å of the low-metallicity component with increasing metallicity of the main SSP component. It becomes largest at $Z \approx Z_{\odot}$, to decrease slightly at higher metallicities, where more flux is emitted at the near-infrared wavelengths (see M98). Models with broader metallicity distributions (for example, the closed box one) smear out this effect, resulting in CaT* and CaT indices steadily increasing with metallicity. The CSP models match the upper third of the galaxy distribution; however, on average they produce CaT* and CaT indices still ≈0.5 Å larger than the observed ones. As discussed in MT, a low-metallicity tail is expected in the projected line-of-sight metallicity distribution, if radial metallicity gradients are present. This is suggested by the analysis of the Lick indices (Davies, Sadler, & Peletier 1993; Mehlert et al. 2000) and color gradients (Saglia et al. 2000). A "halo-like" low-metallicity population could also be in place, reminiscent of the bimodal (color) distributions observed in the globular cluster systems of many giant elliptical galaxies (Larsen et al. 2001 and references therein). Finally, we note that CSP models with a young, metal-rich component, postulated to explain the observed high central Hβ values of some elliptical galaxies (De Jong & Davies 1997) do not help here, since at high metallicities the SSPs predict increasing values of the CaT* and CaT indices with decreasing ages.

To conclude, none of the discussed options alone seem able to explain the observed distribution of the calcium triplet values, and a combination of them might be at work. In particular, it could be that Ca is in fact underabundant in elliptical galaxies.

R. P. S. acknowledges the International Research Exchange fellowship that made possible his visit to the Research School of Astronomy and Astrophysics of the Australian National University in Canberra, where part of the research project described here was performed. R. P. S., R. B., C. M., and D. T. acknowledge the support by the DFG grant SFB 375. We thank S. Edwards, C. Harrison, and L. Pittroff for helping during the observations and data reduction. We acknowledge the discussion with Laura Greggio. We acknowledge the observatories that supported this project: Calar Alto (Centro Astrofisico Hispano Alemano), Siding Spring (MSSSO), and La Silla (ESO).

REFERENCES

Armandroff, T. E., & Zinn, R. 1988, AJ, 96, 92
Bender, R. 1990, A&A, 229, 441
Bender, R., Burstein, D., & Faber, S. M. 1993, ApJ, 411, 153
Bender, R., Saglia, R. P., & Gerhard, O. 1994, MNRAS, 269, 785
Carter, D., Visvanathan, N., & Pickles, J. 1986, ApJ, 311, 637
Cenarro, A. J., Cardiel, N., Gorgas, J., Peletier, R. F., Vazdekis, A., & Prada, F. 2001a, MNRAS, 326, 959 (C01)
Cenarro, A. J., Gorgas, J., Cardiel, N., Pedraz, S., Peletier, R. F., & Vazdekis, A. 2001b, MNRAS, 326, 981
Cenarro, A. J., Gorgas, J., Cardiel, N., Vazdekis, A., & Peletier, R. F. 2002, MNRAS, 329, 863 (C02)
Cohen, J. G. 1979, ApJ, 228, 405
Colless, M., Burstein, D., Davies, R. L., McMahan, R., Saglia, R. P., & Wegner, G. 1999, MNRAS, 303, 813
Couture, J., & Hardy, E. 1993, ApJ, 406, 142
Davies, R. L., Sadler, E. M., & Peletier, R. 1993, MNRAS, 262, 650
De Jong, R. S., & Davies, R. L. 1997, MNRAS, 285, L1
Díaz, A. I., Terlevich, E., & Terlevich, R. 1989, MNRAS, 239, 325
Faber, S. M., & French, H. B. 1980, ApJ, 235, 405
Faber, S. M., Wegner, G., Burstein, D., Davies, R. L., Dressler, A., Lynden-Bell, D., & Terlevich, R. 1989, ApJS, 69, 763 (F89)
García-Vargas, M. L., Mollá, M., & Bressan, A. 1998, A&AS, 130, 513
Gerhard, O., Kronawitter, A., Saglia, R. P., & Bender, R. 2001, AJ, 121, 1936
Harris, W. E. 1996, AJ, 112, 1487
Idiart, T. P., Thévenin, F., & De Freitas Pacheco, J. A. 1997, AJ, 113, 1066 (I97)
Kauffmann, G. 1996, MNRAS, 281, 487
Larsen, S. S., Brodie, J. P., Huchra, J. P., Forbes, D. A., & Grillmair, C. J. 2001, AJ, 121, 2974
Larson, R. B. 1974, MNRAS, 173, 671
Maraston, C. 1998, MNRAS, 300, 872 (M98)
Maraston, C., Greggio, L., Renzini, A., Ortolani, A., Saglia, R. P., Puzia, T. H., & Kissler-Patig, M. 2002, A&A, submitted (astro-ph/0209220)
Maraston, C., & Thomas, D. 2000, ApJ, 541, 126 (MT)
McWilliam, A. 1997, ARA&A, 35, 503
McWilliam, A., & Rich, R. M. 1994, ApJS, 91, 749
Mehlert, D., Saglia, R. P., Bender, R., & Wegner, G. 1998, A&A, 332, 33
———. 2000, A&AS, 141, 449
Mollá, M., & García-Vargas, M. L. 2000, A&A, 359, 18
Peletier, R. F., Vazdekis, A., Arribas, S., del Burgo, C., García-Lorenzo, B., Gutiérrez, C., Mediavilla, E., & Prada, F. 1999, MNRAS, 310, 863
Rich, R. M., & McWilliam, A. 2000, Proc. SPIE, 4005, 150
Saglia, R. P., Maraston, C., Greggio, L., Bender, R., & Ziegler, Z. 2000, A&A, 360, 911
Terlevich, A. I., & Forbes, D. A. 2002, MNRAS, 330, 547
Terlevich, E., Díaz, A. I., & Terlevich, R. 1990, MNRAS, 242, 271
Thomas, D., Maraston, C., & Bender, R. 2002, MNRAS, submitted (astro-ph/0209250) (TMB)
Trager, S. C., Faber, S. M., Worthey, G., & González, J. J. 2000, AJ, 120, 165
Tripicco, M. J., & Bell, R. A. 1995, AJ, 110, 3035
Vazdekis, A., Peletier, R. F., Beckman, J. E., & Casuso, E. 1997, ApJS, 111, 203
Woosley, S. E., & Weaver, T. A. 1995, ApJS, 101, 181
Worthey, G. 1994, ApJS, 95, 107
Worthey, G., Faber, S. M., & González, J. J. 1992, ApJ, 398, 69
Zoccali, M., Cassisi, S., Bono, G., Piotto, G., Rich, R. M., & Djorgovski, S. G. 2000a, ApJ, 538, 289
Zoccali, M., Cassisi, S., Frogel, J. A., Gould, A., Ortolani, S., Renzini, A., Rich, R. M., & Stephens, A. W. 2000b, ApJ, 530, 418